Interplay of resonant cavity modes with localized surface plasmons: optical absorption properties of Bragg stacks integrating gold nanoparticles

Olalla Sánchez-Sobrado,[1] Gabriel Lozano,[1] Mauricio E. Calvo,[1] Ana Sánchez-Iglesias, Luis M. Liz-Marzán,[2,] Hernán Míguez[1,*]*

1. *Instituto de Ciencia de Materiales de Sevilla (Consejo Superior de Investigaciones Científicas-Universidad de Sevilla), C/Américo Vespucio 49, 41092 Sevilla, Spain. hernan@icmse.csic.es*
2. *Departamento de Química Física, and Unidad Asociada CSIC-Universidade de Vigo, 36310 Vigo, Spain. lmarzan@uvigo.es*

Abstract

The optical properties of gold nanoparticles were modulated through integration in one dimensional photonic crystals made of silica and titania nanoparticles. Silica coated gold colloids were used to create a controlled optical defect buried within a periodic multilayer. Matching of the cavity mode with different spectral regions of the localized surface plasmon resonance yields a fine control over the effective absorption of the ensemble. This was achieved by varying the structural parameters of the multilayer. We also demonstrate that subtle environmental changes have dramatic effects on the optical absorption properties of the ensemble. Our work experimentally demonstrates that designed photonic structures can be used to spectrally tune the absorption peak characteristic of metal colloids.

Introduction

Enhancement and confinement of the electromagnetic field at length scales on the order of nanometers constitutes the subject of plasmonics,[1] which finds in metal nanoparticles a platform to study both fundamental phenomena[2] and potential applications in fields like catalysis,[3] energy,[4] sensing[5] or optics.[6] One of the more characteristic features of metal particles is a well-defined resonant optical absorption peak at visible wavelengths caused by the excitation of localized surface plasmons.[7] Such enhanced electromagnetic modes are particle size and shape-dependent and are confined in the boundary between a metallic bead and its dielectric environment, thus being also extremely sensitive to the refractive index of the surrounding medium.[8] This latter property actually makes them suitable as base materials to be use in detection of chemical or biological compounds.[9] At the same time, it implies that some type of coating is needed to stabilize their optical response versus environmental changes, which has boosted active research in methods to obtain core-shell structures, in which the outer layer is typically a dielectric material.[10] Once plasmonic interactions between neighboring particles are screened by a dielectric shell, the color of the metallic particle will depend exclusively on its size and shape, and these are actually the means commonly employed to control their absorption.

From a different perspective, in recent years, the interplay between plasmonic and photonic resonances has gathered considerable attention. A significant number of methods have been developed to incorporate metallic particles, mainly made of gold, into periodic structures.[11-17] In the vast majority of cases, their integration has been achieved by infiltration into three-dimensional self-assembled photonic crystals, the effect of the metal guest being the tuning or enhancement of the reflection peaks (transmission dips) caused by the presence of a photonic stop band in such structures. Also, enhancement of the non-linear Kerr effect, that is, the variation of the refractive index with the squared electric field intensity, has also been observed in thick gold nanoparticle coatings of Bragg stacks.[18] In these one-dimensional photonic crystals the metallic layer acts as an outer defect in which the electromagnetic field is partially localized, which is at the origin of the detected enhancement. Also, intense variations of the optical absorption have been predicted for both one[19]- and two[20]-dimensional periodic structures containing arrays of noble metal particles. In spite of all these

efforts, no experimental studies report on the controlled tuning and enhancement of the absorption properties of hybrid plasmonic-photonic materials as a result of the enhanced field localization in the vicinity of metal particles. The reason for this is probably the weak localization effects observed in three dimensional self-assembled photonic crystals, in which both dielectric contrast and the degree of order are low, or the difficulty to embed the metallic particles in actual optical resonators in which the localization effects are stronger.

Herein we demonstrate that the interplay between localized surface plasmons in gold nanoparticles and the field confinement effects occurring in optical resonators containing them leads to selective spectral enhancement and fine tuning of the optical absorption of the ensemble. Silica coated gold particles were integrated as a controlled defect layer into periodic stacks of nanoparticles with one dimensional photonic crystal properties to achieve the materials subject of this study. Also, the porous character of the final hybrid material is taken advantage of to analyze the dependence of the absorption spectrum upon the presence of different types of liquid compounds in the void network, which yields a precise response as a function of the refractive index of the guest.

Results and discussion

Stabilized gold nanoparticles used in our study were prepared following a well-established and generic procedure that has been thoroughly described before.[21] The particles present a gold core of 6.5 nm radius and a silica corona of 16 nm thickness, as can be seen in the transmission electron micrograph displayed in Figure 1(a), and we label them as Au@SiO_2 particles. This coating was chosen since it has been shown that a 15 nm thick silica layer is enough to both screen the plasmonic interactions between neighboring gold cores and remove the dependence of the extinction spectra on the dielectric constant of the surrounding medium.[10] This was experimentally confirmed by comparing the visible extinction spectra of a suspension of Au@SiO_2 particles and that of a thin layer of them (Figures S1 and S2 respectively of the Supplementary information).

Optical resonators integrating metallic particles were built by introducing a middle layer of gold nanoparticles within one-dimensional photonic crystals comprising alternate layers of controlled thickness, made of silica and titania nanoparticles, which were

deposited on flat glass substrates following a previously reported procedure.[22] A representative cross section image of one of these ensembles is shown in Figure 1(b). The larger size of the spherical core-shell particles sandwiched within the two periodic multilayers does not alter the long range order of the structure. This adaptability is a characteristic feature of Bragg stacks made of nanoparticles. Smaller TiO_2 nanocrystals create a layer of uniform thickness when deposited onto a rougher surface. This feature has been demonstrated in optical resonators integrating large rare earth particles of rhombohedral shape, in which enhancement or suppression of selected luminescence emission lines was achieved.[23]

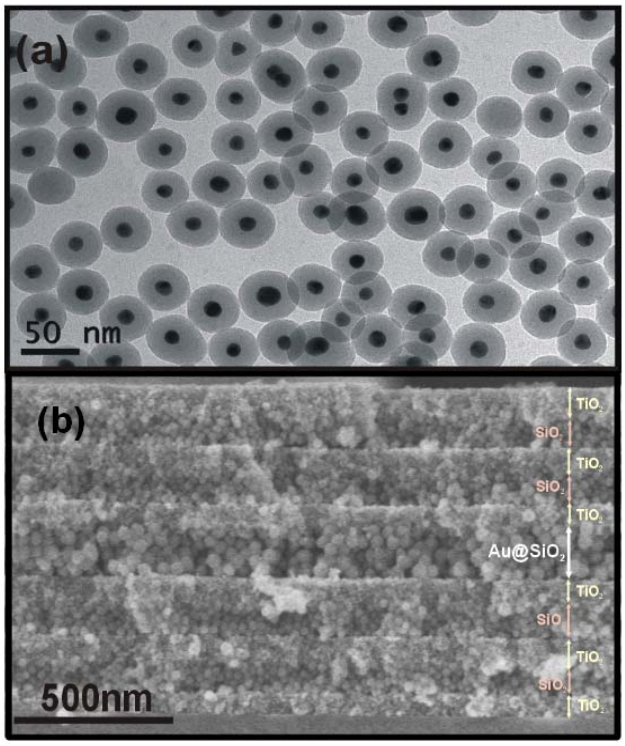

Figure 1. (a) Representative TEM image of the $Au@SiO_2$ core-shell particles employed in this work. (b) Representative SEM image of a cross section of a one-dimensional SiO_2-TiO_2 nanoparticle photonic crystal in which a middle layer of $Au@SiO_2$ nanoparticles was embedded.

Optical characterization was carried out using a spectrophotometer attached to an integrating sphere operating in both total reflection and total transmission modes (both configurations are illustrated in Figures S3(a) and S3(b), respectively, of the Supporting

Information). Extreme care was taken to collect all reflected and transmitted light (that is, the specularly reflected and ballistically transmitted beams, as well as the forward and backward diffuse light) from precisely the same area of the crystal, as well as to minimize losses caused by geometrical constraints of the device employed. Independent measurements made using a specular reflectance set-up show that diffusely scattered light accounts for less than 5% of the total scattered light, indicating that the multilayers present a low density of imperfections.

Representative results for one of the multilayers are shown in Figure 2. It can be clearly seen in Figure 2(a) that total reflectance (R_T, black curve) and total transmittance (T_T, red curve) display the typical spectral features of an optical resonator. The buried Au@SiO_2 layer acts as an optical defect that breaks the translational symmetry of the stack, thus giving rise to electromagnetic modes localized within the layer. In this example, the intensity reflected by the multilayers is maximum for 450 nm <λ<750 nm, and the transmission window caused by the resonant cavity mode opens up at around 535 nm (see vertical grey line). Optical absorptance, A, was calculated from the total reflectance and transmittance measurements using the formula $A=1-R_T-T_T$. The result is plotted in Figure 2b for the resonator containing Au@SiO_2 particles (orange curve), for a resonator with similar spectral features but without metal particles (green curve), which was used as a test of the reliability of our measurements, and for a reference layer of Au@SiO_2 particles of the same thickness (as confirmed in the FESEM, see Figure S1), deposited on a thin film of TiO_2 nanoparticles (black curve). The resonator used as a blank shows a nearly flat spectrum, which allow us estimating the absolute absorptance measurement error to be always less than 3% (see Supplementary Information, Figure S4). For the optical resonator containing Au@SiO_2 particles, maximum absorption is now centered at a wavelength that coincides with the resonant mode of the optical cavity (as indicated by the vertical grey line), with an absorptance intensity that is almost double than that in the reference. The absorptance peak is slightly red-shifted with respect to that measured from the reference layer. It should also be noted that absorption of light with wavelength within the photonic band gap but off-resonance is lower that in the reference layer, which is due to the screening effect of the photonic crystal mirror. This example illustrates well the effects arising from the interplay between the optical cavity and the intrinsic localized surface plasmon

resonance of the Au@SiO_2 particles, i.e. spectral shift and selective enhancement of the absorption by the metallic particles.

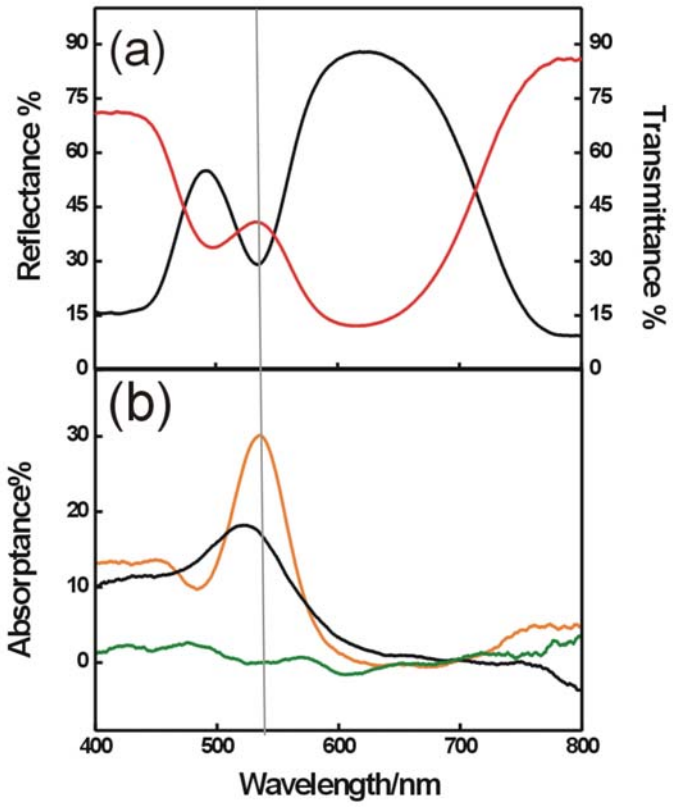

Figure 2. (a) Total reflectance (black curve) and total transmittance (red curve) spectra of an optical cavity made of Au@SiO_2 nanoparticles sandwiched between two one-dimensional photonic crystals. (b) Optical absorptance spectrum of the resonator (orange curve), compared to that of a layer of Au@SiO_2 nanoparticles of similar thickness (black curve) and that of a resonator containing no metal or absorbing particles (green curve), which we used as a blank. The vertical grey line indicates the spectral position of the cavity resonance.

Further evidence of the effect of this interplay was achieved by infiltrating the porous network of the photonic crystal with liquids of different refractive index *n*. As it has been demonstrated earlier,[22] this causes an effective red-shift of the optical cavity resonance. Isopropanol (*n*=1.377), toluene (*n*=1.497) and chlorobenzene (n=1.525) were employed. For the sake of clarity, only the total reflectance spectra recorded after each infiltration are displayed in Figure 3a, but full reflectance and transmittance spectra can be consulted in the supporting information (Figure S5). Absorptance spectra are shown

in Figure 3b. It can be clearly observed that upon infiltration of the pores, the absorptance spectra display a double peak structure, as a consequence of two different enhancement effects that occur simultaneously. On one hand, photon modes with wavelength matching that of the cavity resonance are localized at the Au@SiO_2 layer, thus increasing their absorption (see vertical lines in Figure 3). As the refractive index of the pores increases when liquid is infiltrated, this phenomenon takes place at longer wavelengths, as seen in Figure 3b. At the same time, since the whole photonic crystal is porous, the Bragg peak is red-shifted and at some point its higher energy edge will also match the absorption band of the Au@SiO_2 particles. Those photon modes will be preferentially localized within the lower dielectric constant layers of the stack, including the Au@SiO_2 mid-layer, hence providing a second source of absorptance enhancement. Further analysis of this band edge enhancement effect is presented as supplementary information. In Figure 3(c), we plot the fitting of two of the absorptance spectra measured from the multilayers under analysis. A longer description of the calculation methods[24] and parameters[25] used to of perform these simulations is provided in the supplementary information. Using these same theoretical tools, we calculated the spatial distribution of the squared electric field along a cross section of the photonic crystal embedding an optical cavity made of Au@SiO_2 nanoparticles for different wavelengths. It can be readily identified in Figure 4, where results are presented, regions where field intensity is enlarged or reduced. All selective absorption reinforcement phenomena observed are due to preferential confinement of the resonant electromagnetic modes within the layers containing Au@SiO_2 nanoparticles. In few words, the increase of the photon density of states caused by confinement in specific slabs of the multilayer implies a lower group propagation velocity for those modes,[26] which in turn yields longer light-matter interactions and thus a higher probability of absorption.[27] On the contrary, reduction of the field intensity in selected regions gives rise to weaker interactions, hence to lower probability of absorption.

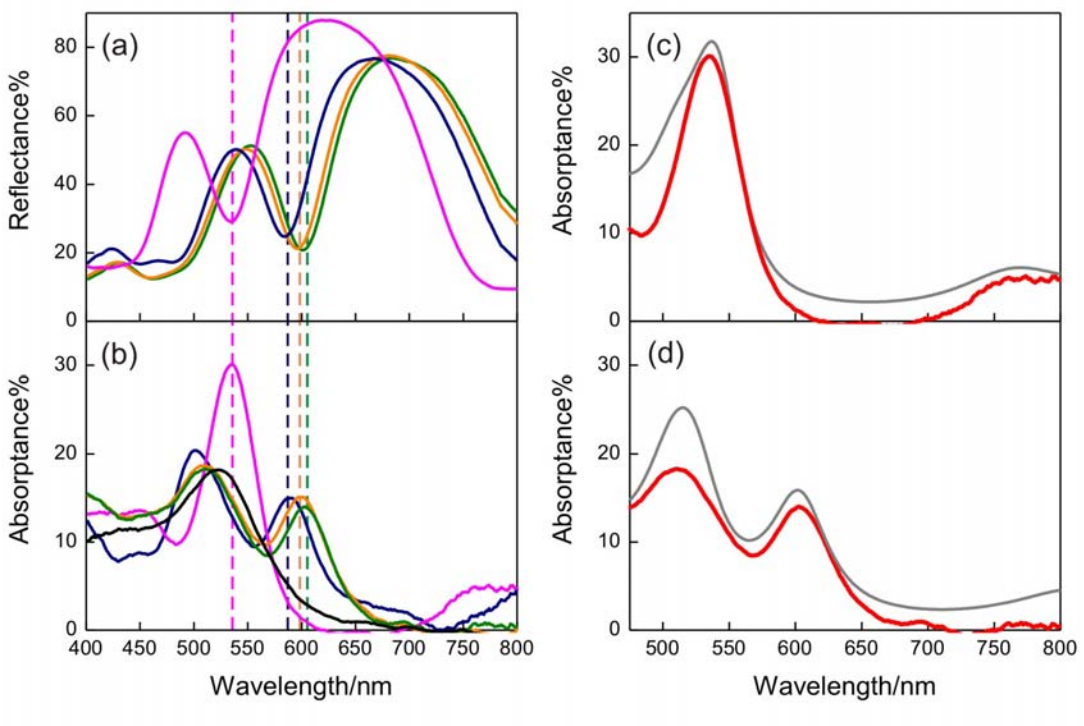

Figure 3. (a) Total reflectance spectra of an optical cavity made of Au@SiO_2 nanoparticles sandwiched between two one-dimensional photonic crystals before (magenta curve) and after being infiltrated with isopropanol (*n*=1.377, blue curve), toluene (*n*=1.497, orange curve) and chlorobenzene (n=1.525, green curve). (b) The corresponding optical absorptance spectra (same color code). Vertical lines indicate the spectral position of the cavity resonance in each case. The optical absorptance spectrum of a layer of Au@SiO_2 nanoparticles of similar thickness is also shown as a reference (black curve). (c) and (d) display experimental (red curves) and calculated (black curves) absorptance spectra of (c) a multilayer containing a mid-layer of Au@SiO_2 nanoparticles acting as an optical cavity and of (d) the same structure after being infiltrated with chlorobenzene (n=1.525).

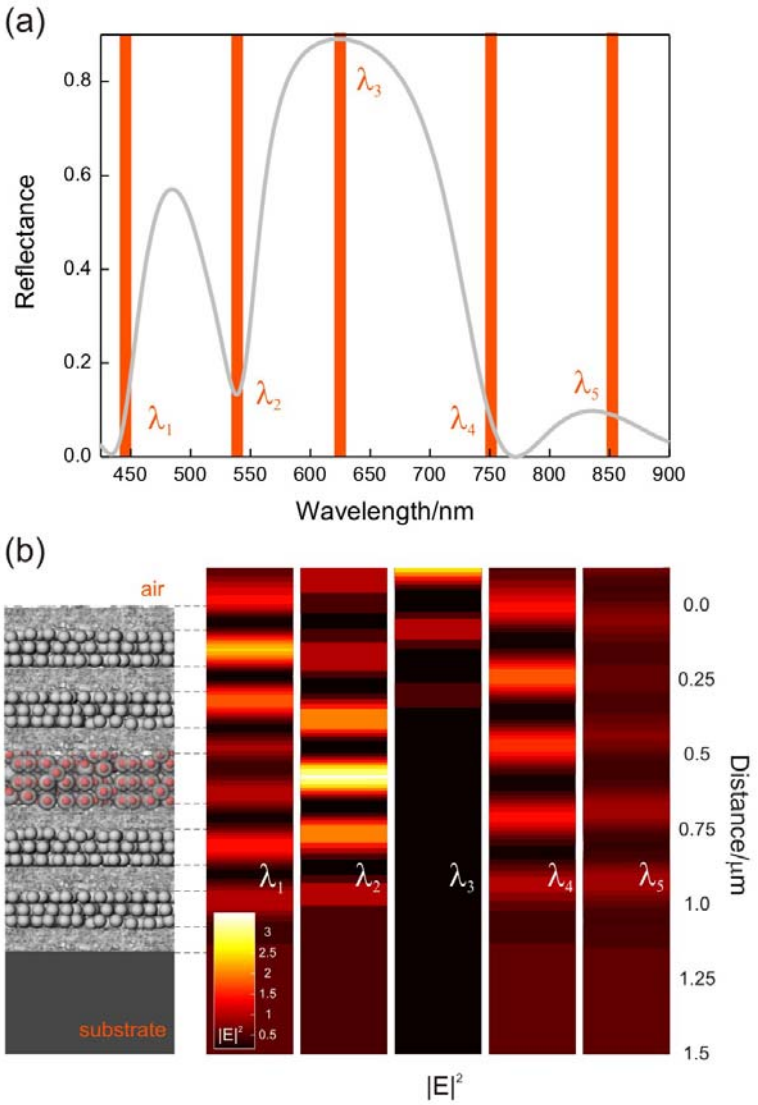

Figure 4. (a) Calculated specular reflectance of a multilayer with similar structural parameters to those obtained experimentally. Vertical bars indicate the spectral position of photon modes located at the blue-edge of the photonic band gap (λ_1), the center of the resonance (λ_2), the center of the photonic band gap (λ_3), the red-edge of the photonic band gap (λ_4), and the passband of the photonic crystal (λ_5). (b) Left panel shows a model of the simulated structure, where Au@SiO_2 particles are represented by grey spheres with red core. Panels on the right show the calculated spatial distribution of the squared magnitude of the electric field along a cross section of the multilayer for all wavelengths highlighted in the reflectance spectrum shown in Figure 4(a). A color intensity scale is provided.

Conclusions

In conclusion, we have shown that the interplay between localized surface plasmons of gold nanoparticles and the field confinement effects occurring in optical resonators containing them can be used to achieve spectrally selective enhancement of the optical absorption of the ensemble. We have also demonstrated that the porous nature of the final hybrid material provides a means to precisely control the absorption spectrum of the multilayer as a function of the refractive index of guest compounds. These novel hybrid plasmonic-photonic materials might provide new ways of controlling the optical response stemming from localized surface plasmon resonances in metal particles.

Experimental

Preparation of nanoparticle colloids

Au@SiO_2 nanoparticles were synthesized by a previously reported method.[21] In brief, a silane coupling agent (3-aminopropylmethoxysilane) was used to make the surface of the gold particles vitreophilic. When put into contact with silicate anions at pH close to 8, the silane modified particles were coated by a homogeneous silica shell that allowed transfer to ethanol. The final thickness of the silica shell was controlled by subsequent growth by basic hydrolysis and condensation of tetraethoxysilane in an ethanol/ammonia mixture. The sample used here contained Au@SiO_2 nanoparticles with a core diameter of 13 nm and a 16 nm shell thickness, with a concentration of 2 wt% in methanol, adjusted by centrifugation and redispersion.

TiO_2 nanoparticulated sols were synthesized using a procedure based on the hydrolysis of titanium tetraisopropoxide ($Ti(OCH_2CH_2CH_3)_4$, 97% *Aldrich*, abbrev. TTIP) as it previously described.[22] Briefly, TTIP was added to Milli-Q water, the white precipitate filtered and washed several times with distilled water. The resulting solid was peptized in an oven at 120º C for 3 hours with tetramethylammonium hydroxide (*Fluka*). Finally, the suspension was centrifuged at 14,000 rpm for 10 min. SiO_2 nanocolloids were purchased from Dupont (LUDOX TMA, *Aldrich*). Both suspensions were diluted in methanol with concentrations

between 2 wt.% and 4 wt.% and then filtered using syringe driven filters (*Millipore*) of 0.45 μm and 0.22 μm for 30 nm diameter SiO_2 and 13 nm diameter TiO_2 particles, respectively.

Preparation of one-dimensional photonic crystals containing Au@SiO_2 nanoparticles

Photonic crystals were built by alternate deposition of TiO_2 and SiO_2 nanoparticulated suspensions, following a generic procedure previously reported.[22] These sols were deposited over zero fluorescence glass (Proscitech) using a spin coater (Laurell WS-400E-6NPP) in which both the acceleration ramp and the final rotation speed could be precisely determined. The first layer was deposited using 200 μL of TiO_2 sol and the substrate was tilted and rotated to let the suspension cover the total glass surface. Then, the sample was accelerated up to different final speed, in order to control the thickness of each layer. TiO_2 and SiO_2 layers were deposited at 3000 rpm with an acceleration of 11340 rpm s^{-1}. The spin-coating process was completed in 60 s. Subsequently, another layer of a different type of nanoparticle was deposited following the same procedure. The process was repeated until a final number of layers forming each sample has been deposited. The layers of Au@SiO_2 nanoparticles were introduced in the middle of the stacks by spin-coating 200 μL drops of a 1.45 wt. % suspension in methanol using a final speed in the range 3000-7000 rpm, with a fixed acceleration ramp of 11340 rpm s^{-1}. The samples used as reference were deposited following similar conditions.

Characterization

Total reflectance and total transmittance spectra were obtained using a UV-visible scanning spectrophotometer (SHIMADZU UV-2101PC) attached to an integrating sphere. Specular reflectance was also obtained for comparison using a Fourier Transform IR spectrophotometer (Bruker IFS-66 FTIR) attached to a microscope and operating in reflection mode with a 4× objective with numerical aperture 0.1 (light cone angle ±5.7º). TEM images were recorded with a JEOL JEM 1010 transmission electron microscope operating at an acceleration voltage of 100 kV. FESEM cross section images of the films were taken with a Hitachi S-4800 microscope operating at 2 kV.

Acknowledgements

We thank the Spanish Ministry of Science and Innovation for funding provided under grants MAT2008-02166 and CONSOLIDER HOPE CSD2007-00007, to Junta de Andalucía for grants FQM3579 and FQM5247. MEC thanks the Junta de Andalucía for funding of his contract. LML-M acknowledges financial support from MiCInn/FEDER (MAT2007-62696) and Xunta de Galicia (09TMT011314PR).

References

[1] E. Ozbay, *Science* **2006**, *311*, 189.

[2] P. V. Kamat, *J. Phys. Chem. B* **2002,** *106*, 7729.

[3] R. M. Crooks, M. Zhao, L. Sun, V. Chechik, L. K. Yeung, *Acc. Chem. Res.* **2001**, *34*, 181.

[4] H. A. Atwater, A. Polman, *Nat. Mater.* **2010**, *9*, 124.

[5] D. J. Maxwell, J. R. Taylor, S. Nie, *J. Am. Chem. Soc.* **2002**, *124*, 9606.

[6] E. Hutter, J. H. Fendler, *Adv. Mater* **2004**, *16*, 1685.

[7] S. Link, M. A. El-Sayed, *J. Phys. Chem. B* **1999,** *103*, 8410

[8] K. L. Kelly, E. Coronado, L. L. Zhao, G. C. Schatz, *J. Phys. Chem. B* **2003**, *107*, 668.

[9] K. A. Willets, R. P. Van Duyne, *Ann. Rev. Phys. Chem.* **2004**, *58*, 267.

[10] L. M. Liz-Marzán, P. Mulvaney, *J. Phys. Chem. B* **2003,** *107*, 7312.

[11] F. García-Santamaría, V. Salgueirino-Maceira, C. López, L. M. Liz-Marzán, *Langmuir* **2002**, *18*, 4519.

[12] D. Y. Wang, V. Salgueiriño-Maceira, L. M. Liz-Marzán, F. Caruso, *Adv. Mater.* **2002**, *14*, 908.

[13] D. Y. Wang, J. Li, C. T. Chan, V. Salgueiriño-Maceira, L. M. Liz-Marzán, S. Romanov, F. Caruso, *Small* **2005**, *1*, 122.

[14] J. Wang, S. Ahl, Q. Li, M. Kreiter, T. Neumann, K. Burkert, W. Knoll, U. Jonas, *J. Mater. Chem.* **2008**, *18*, 981.

[15] D. Yu, M. C. George, P. V. Braun, *J. Amer. Chem. Soc.* **2010**, *132*, 9958.

[16] S. Shukla, A. Baev, H. Jee, R. Hu, R. Burzynski, Y. K. Yoon, P. N. Prasad, *ACS Appl. Mater. Inter.* **2010**, *4*, 1242.

[17] M. Barth, S. Schietinger, S. Fischer, J. Becker, N. Nuesse, T. Aichele, B. Loechel, C. Soennichsen, O. Benson, *Nano Lett.* **2010**, *10*, 891.

[18] H. Inouyea, Y. Kanemitsu, *Appl. Phys. Lett.* **2003**, *82*, 1155.

[19] E. Lidorikis, S. Egusa, and J. D. Joannopoulos, *J. Appl. Phys.* **2007**, *101*, 054304.

[20] H. Jiang, J. Sabarinathan, T. Manifar, S. Mittler, *IEEE J. Light. Tech.* **2009**, *27*, 2264.

[21] L. M. Liz-Marzán, M. Giersig, P. Mulvaney, *Langmuir* **1996**, *12*, 4329.

[22] S. Colodrero, M. Ocaña, H. Míguez, *Langmuir* **2008**, *24*, 4430.

[23] O. Sanchez-Sobrado, M. E. Calvo, N. Nuñez, M. Ocaña, G. Lozano, H. Míguez, *Nanoscale* **2010**, *2*, 936.

[24] G. Lozano, S. Colodrero, O. Caulier, M. E. Calvo, H. Míguez, *J. Phys. Chem. C.* **2010**, *114*, 3681.

[25] T. Ung, L. M. Liz-Marzán, P. Mulvaney, *J. Phys. Chem. B* **2001**, 105, 3441.

[26] J. M. Bendickson, J. P. Dowling, M. Scalora, *Phys. Rev. E* **1996**, *53*, 4107.

[27] N. A. R. Bhat, J. E. Sipe, *Phys. Rev. E* **2001**, *64*, 056604.

Supporting information

Confirmation of the screening effect of interparticle interactions by the silica coating

In order to confirm the screening of the interparticle interactions caused by presence of a silica coating on the gold particles, we deposited a layer of $Au@SiO_2$ nanoparticles onto a flat glass substrate. The visible extinction spectra of the precursor colloidal suspension containing the $Au@SiO_2$ particles in a concentration of 2 vol. % was compared with that of a 250 nm thick layer deposited from it and that of the same layer with its void network infiltrated with isopropanol (refractive index n=1.38). We found that the absorption peaks occur at the same spectral position in all three cases, demonstrating the efficient screening effect of the silica coating. Similar layers were prepared to be used as references for all the conducted optical studies. The cross section of a typical reference sample as seen in the field emission scanning electron microscope (FESEM) as well as the optical absorption spectra of suspended particles as well as of both deposited and solvent infiltrated layers are shown in Figures S1 and S2.

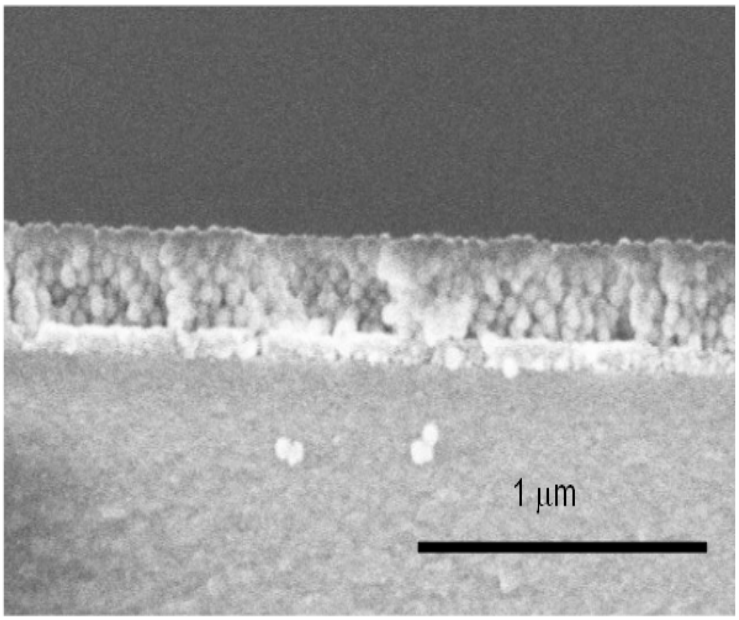

Figure S1. Scanning electron microscopy image of a cross section of a layer of $Au@SiO_2$ particles deposited by spin-coating the precursor suspension on a thin TiO_2 nanoparticle film, which was in turn deposited on glass. Similar layers were used as reference samples for the optical characterization experiments.

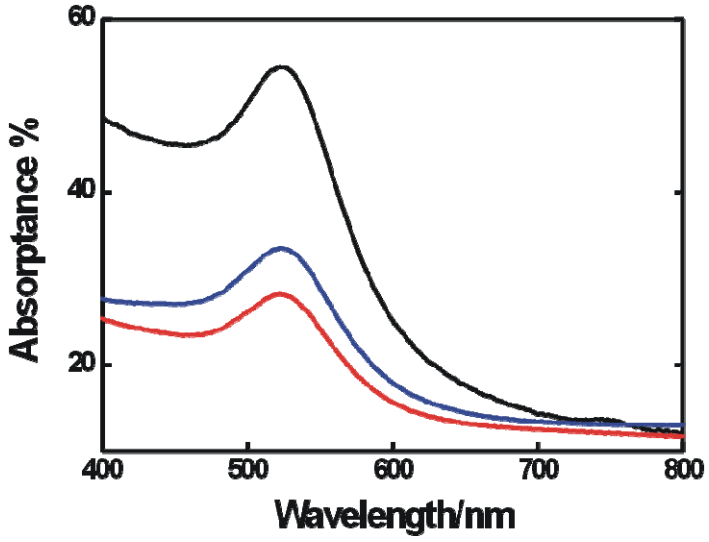

Figure S2. Absorptance of the Au@SiO_2 nanoparticle suspension (black curve) and of a 200 nm thick layer of the same particles deposited on glass before (blue) and after (red) being infiltrated with isopropanol.

Experimental set-up used to measure total transmittance and total reflectance and examples of registered spectra.

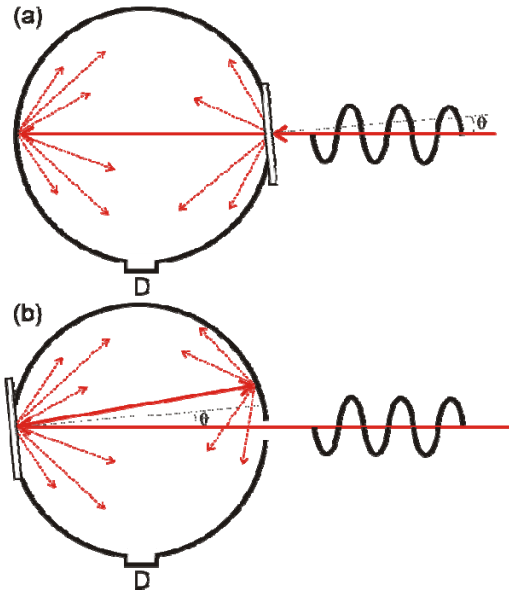

Figure S3. Schemes of the geometry employed to detect (a) total transmitted and (b) total reflected light. The incident angle θ (5º) was enlarged for the sake of clarity. The sample is represented by a thin rectangle and D stands for detector.

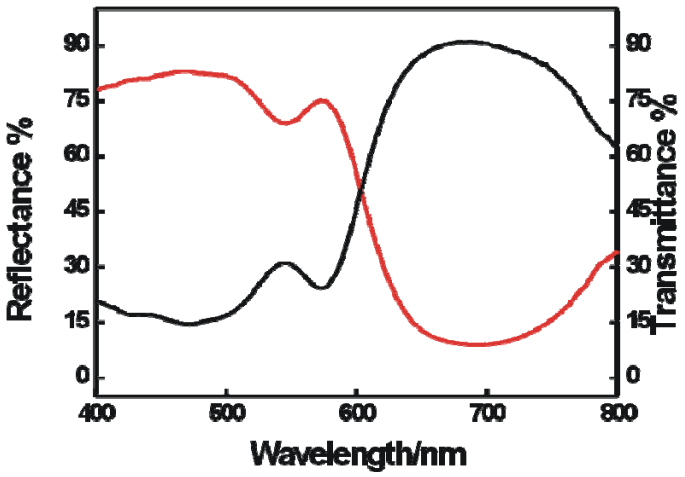

Figure S4. Reflectance (black line) and transmittance spectra (red line) of the resonator used as a blank, i.e. not containing any Au@SiO_2 particles. The absorptance spectrum plotted in green color shown in Figure 5 results from adding these two spectra and subtracting it from one.

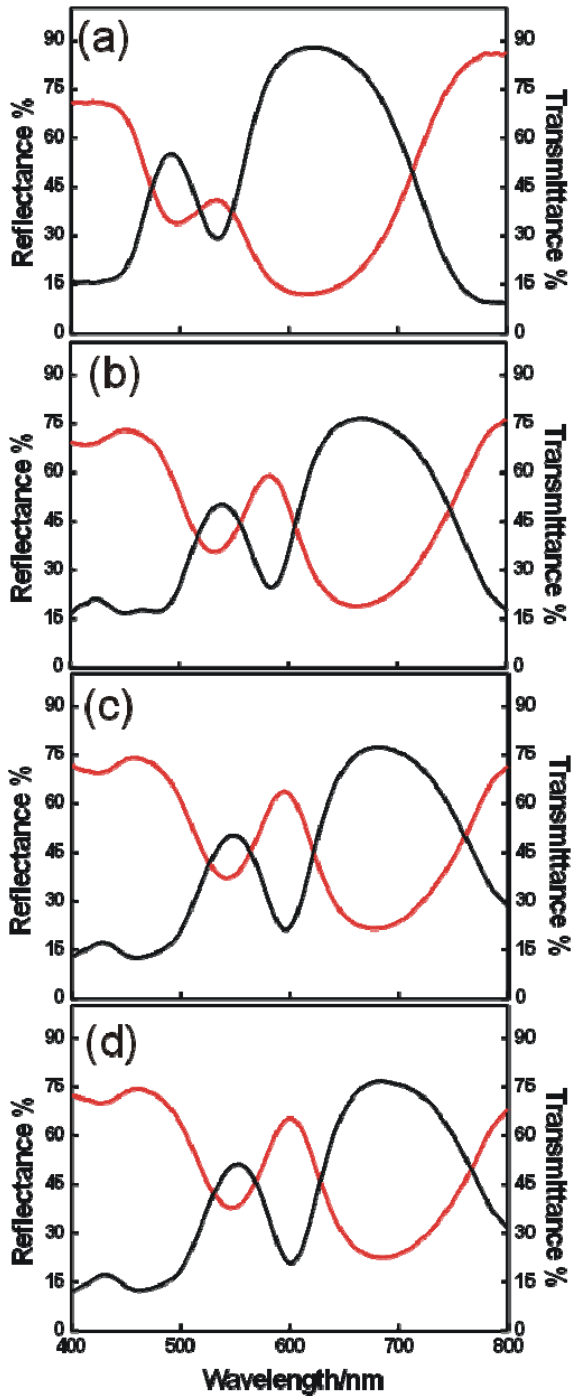

Figure S5. Reflectance (black curves) and transmittance (red curves) spectra of an optical resonator containing a mid-layer Au@SiO_2 particles (a) before and after being infiltrated with and after being infiltrated with (b) isopropanol (*n*=1.377), (c) toluene (*n*=1.497) and (d) benzene (n=1.525). These spectra were used to obtain the absorptance spectra shown in Figure 7(b).

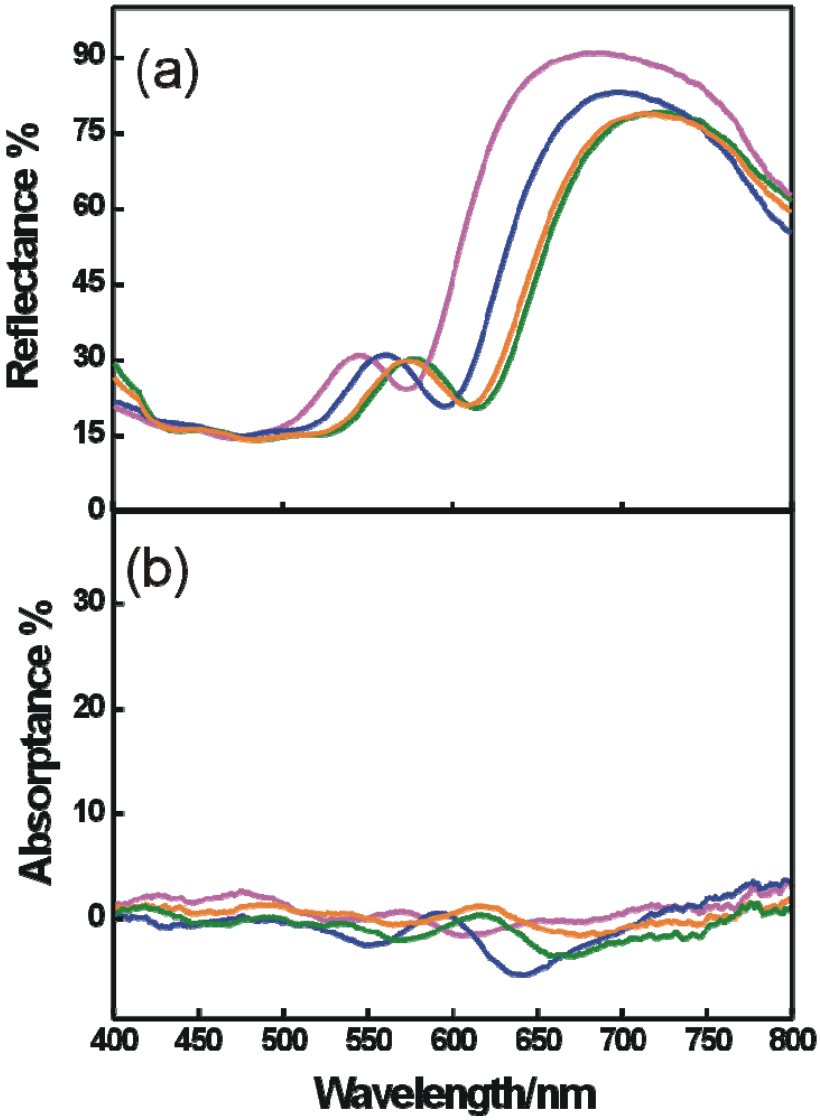

Figure S6. (a) Reflectance and (b) absorptance spectra of a standard photonic crystal without Au@SiO_2 nanoparticles before (magenta curve) and after being infiltrated with isopropanol (*n*=1.377, blue curve), toluene (*n*=1.497, orange curve) and benzene (n=1.525, green curve). No reinforcement effect is detected at blue-edge nor at red-edge frequencies, as expected.

Further analysis of the absorptance enhancement effect at photonic band gap blue edge.

Further analysis of this band edge enhancement effect was attained from samples in which one of the silica layers was substituted by a layer of $Au@SiO_2$ nanoparticles but designed so that no optical cavity mode was created. This was achieved by controlling the optical thickness, resulting from multiplying its thickness by its average refractive index, of the middle layer of $Au@SiO_2$ nanoparticles so that it was similar to the remaining silica layers in the multilayer. In this case, the only source of absorption increase is the coincidence between the optical absorption of the gold particles and the blue-edge of the photonic band gap. Total optical reflectance and absorptance spectra are displayed in Figure 4 for the as prepared multilayer before (magenta curves) and after being infiltrated with isopropanol (blue curves), toluene (orange curves) and benzene (green curves). The blue-edge shift and enhancement effect on the absorptance spectra can be readily seen. No reinforcement effect is detected at the red-edge frequencies, for which the electric field is concentrated within the higher refractive index TiO_2 layers.

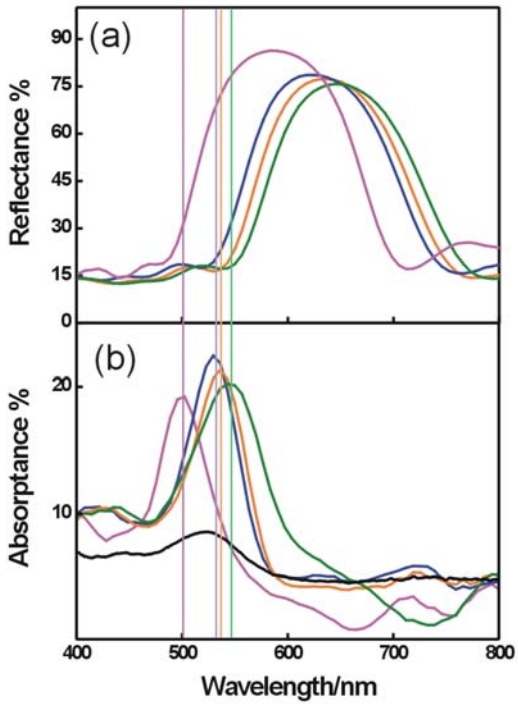

Figure S7. (a) Reflectance and (b) absorptance spectra of a photonic crystal in which one of the constituent silica layers has been substituted by a 100 nm thick layer of $Au@SiO_2$ nanoparticles before (magenta curve) and after being infiltrated with isopropanol (n=1.377, blue curve), toluene (n=1.497, orange curve) and benzene (n=1.525, green curve). Vertical lines indicate the spectral position of the blue-edge in each case.

Description of the calculation methods and deeper analysis of Figure 4.

Theoretical calculations were performed using a transfer matrix approach,[26] as described earlier and using reported optical data for $Au@SiO_2$ nanoparticles.[27] Results were drawn for wavelengths: λ_1, located at the blue-edge of the photonic band gap; λ_2, at the optical resonance, for which the dip is observed in the reflectance spectrum; λ_3, within the photonic band gap and for which reflectance is maximum; λ_4, at the red-edge of the photonic band gap; and λ_5, in the pass-band of the photonic crystal. All these wavelengths are highlighted in the reflectance spectrum plotted in Figure 4(a). It can be clearly seen in the field distribution patterns plotted in Figure 4(b) that light localizes preferentially within the lower refractive index layers (i.e., silica layers) for λ_1, as expected for a mode in the higher energy band of a photonic crystal. The electric field is even more intensely reinforced within the middle $Au@SiO_2$ layer for λ_2, as expected for a resonant mode of the cavity. These modes show actually the highest absorptance in the experimental results presented. On the contrary, light transmission is blocked for λ_3, thus showing a very short penetration dept, or localized within the higher refractive index non-absorbing titania layers for λ_4, and λ_5, thus a decrease of absorptance is observed. Furthermore, the same model was used to fit the absorptance spectra attained for two particular samples, i.e., the as-prepared optical cavity for which the resonance matches the maximum of the localized surface plasmon absorption peak (see Figure 2) and the same multilayer infiltrated with chlorobenzene (n=1.525, see green curves in Figure 3). Results are displayed in Figures 3(c) and 3(d) respectively. Both the absorption band shape and the reinforcement effects are well-reproduced by our model.